JOURNAL OF GEOPHYSICAL RESEARCH, VOL. 103, NO. A4, PAGES 6685–6692, APRIL 1, 1998

Electron density at the subsolar magnetopause for high magnetic shear: ISEE 1 and 2 observations

D. Hubert and C. C. Harvey

Département de Recherche Spatiale, Observatoire de Paris, Meudon, France

M. Roth and J. De Keyser

Belgian Institute for Space Aeronomy, Brussels

Abstract. The ISEE radio wave propagation electron density experiment allowed the determination of the integrated electron density between the ISEE 1 and ISEE 2 satellites at the relatively high rate of 8 or 32 Hz. When the component of the spacecraft separation vector in the direction of the normal to the magnetopause is significantly smaller than the thickness of the current layer, this data set allows the internal structure of the magnetopause to be studied and compared with theoretical predictions. For a particular triple subsolar magnetopause crossing with high magnetic shear, an electron density overshoot is observed in the current layer adjacent to the magnetosheath. The similarity of the three crossings indicates that the internal structure of the magnetopause does not change dramatically during the time interval considered. A superposed epoch analysis of these crossings is consistent with the density profile obtained from kinetic simulations. The general relationship between magnetic field asymmetry, magnetic field rotation angle and electron density overshoot is discussed. It is concluded that a density overshoot could be a typical feature of the subsolar magnetopause with high magnetic shear. This conclusion is supported by two other dayside magnetopause crossings for which high time resolution electron density data are available.

1. Introduction

The study of the structure and dynamics of the Earth's magnetopause current layer (MCL) is fundamental to understanding the coupling between the solar wind and the magnetospheric environment. The simplest model of the MCL is a tangential discontinuity (TD) within which the magnetic field rotates from an arbitrary interplanetary direction to the magnetospheric direction. The Vlasov kinetic approach has been used in the past to describe the inner structure of the TD magnetopause with different degrees of sophistication [e.g., *Roth*, 1978, 1979; *Lee and Kan*, 1979; *Roth et al.*, 1996]. In recent work by *Kuznetsova and Roth* [1995] (hereafter referred to as the KR model) this approach was used to study the stability of magnetic surfaces with respect to spontaneous excitation of collisionless tearing perturbations within MCLs characterized by large angles of magnetic field rotation θ ($\theta \geq 60°$) and asymmetrical magnetic field profiles. These unperturbed MCLs were also characterized by the absence of shear in the plasma flow, and so they may be typical of the dayside magnetopause near the stagnation point for various orientations of the interplanetary magnetic field (IMF). In the KR model, the structure of the unperturbed asymmetrical MCLs is determined only by the magnetic field rotation angle θ and the magnetic field asymmetry factor $\kappa_B = (B_{\mathrm{msph}} - B_{\mathrm{msh}})/B_{\mathrm{msph}}$, where B_{msph} and B_{msh} are respectively the magnetic field intensities in the adjacent magnetosphere and magnetosheath regions. This model predicts the electron density profile through the unperturbed MCL as a function of the two parameters θ and κ_B. The main characteristic is an enhancement of the electron density in a region of the MCL adjacent to the magnetosheath with a thickness of a few ion Larmor radii; this enhancement decreases with increasing magnetic field asymmetry factor κ_B, but increases with the magnetic field rotation θ [see *Kuznetsova and Roth*, 1995, Figure 2].

To our knowledge, the prediction of an enhancement of the density through the MCL has never been substantiated by observation. The enhancement in the plasma density near the stagnation streamline just in front of the magnetopause observed by *Song et al.* [1990] is a phenomenon inherent to the inner magnetosheath [*Song et al.*, 1992; *Zhang et al.*, 1996]. On the average this structure is about 0.4 R_E thick and clearly separated from the magnetopause. Nevertheless, the analysis of *Song et al.* [1990] displays some events of short duration adjacent to the magnetopause. Although many spacecraft magnetometers can sample the vector magnetic field more than 15 times per second, the plasma velocity distribution functions can not be sampled with comparably high resolution by classical spaceborne particle spec-

Paper number 97JA03298.
0148-0227/98/97JA-03298$09.00

trometers, whose typical interval separating independent density determinations is of the order of 1 s. Observation and analysis of the fine structure of the magnetopause, however, become possible when both plasma and field data have similar high temporal resolution. This requires another technique for measuring plasma parameters. The radio propagation experiment of the Paris Observatory, which determines the mean electron density between the ISEE 1–2 pair of satellites, has a sampling frequency of 8 Hz in low bit rate or 32 Hz in high bit rate, twice that of the magnetometer (4 or 16 Hz, respectively) [*Harvey et al.*, 1978]. Measurements made by this instrument have motivated us to look for observational evidence of the density enhancements predicted by the KR model.

To distinguish the observational properties characteristic of the magnetopause from those characteristic of the inner magnetosheath, we analyze the mean electron density data when the ISEE 1–2 separation distance was small. The radio propagation experiment determines the mean interspacecraft electron density; this is nearly equal to the local density when the distance of separation is significantly lower than the typical wavelength of the density fluctuations; elsewhere, correction factors may be used (D. Hubert et al., Nature, properties, and origin of low-frequency modes from an oblique shock to the inner magnetosheath, submitted to *Journal of Geophysical Research*, 1996). The magnetic field data measured by the UCLA fluxgate magnetometers [*Russell*, 1978] are used to identify the magnetopause crossings. In section 2 we present the observations, which we compare with theoretical model predictions in section 3. The paper ends with a discussion.

2. Observations

Figure 1 shows an overview of the triple crossing of the magnetopause observed by ISEE 1 and 2 on August 30, 1981 (day 242) between 1445 and 1452 UT, when the spacecraft were on the outbound leg of the orbit, near the Sun-Earth line, at a GSM local time of 1235 and a latitude of 1°N. This is close to the stagnation point where the plasma flow on either side of the magnetopause is expected to be small. The magnetopause passed over the spacecraft three times during this interval, at a radial distance of 10.7 R_E from the Earth. The separation between the spacecraft was 260 km, with ISEE 2 leading ISEE 1. Figures 1a–1c display the magnetic field components measured by ISEE 2 (the leading satellite) and Figures 1e–1g those measured by ISEE 1 (the trailing satellite). The fields are displayed in the boundary normal LMN coordinate system [*Russell and Elphic*, 1979] determined near 1450 UT when ISEE 2 was crossing the magnetopause: $\mathbf{n}$ = (0.99, 0.02, 0.12) in GSE coordinates. At 1450 UT the position of ISEE 2 with respect to ISEE 1 was (-118, 78, 220) km in LMN coordinates. The vector magnetic field $\mathbf{B}$ was sampled at 16 Hz.

For each satellite, the three crossings of the magnetopause occur in the time intervals denoted by MP1, MP2 and MP3 in Figure 1. An observational definition of the magnetopause appropriate for the high magnetic shear case is the following:

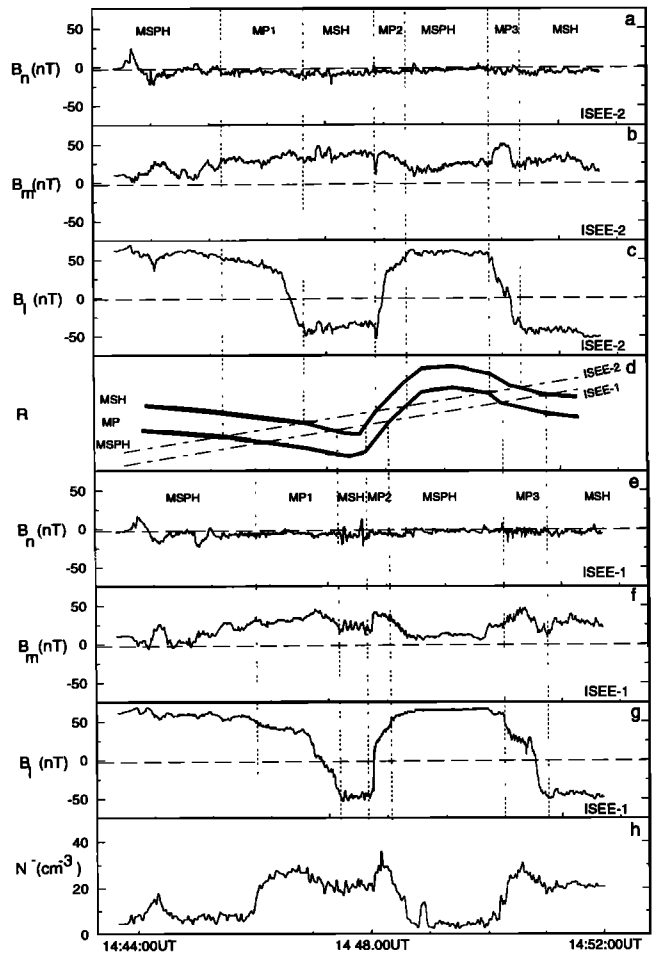

Figure 1. Overview of a multiple magnetopause crossing by ISEE 1 and 2 between 1444 and 1453 UT on August 30, 1981 (day 242). (a–c) LMN magnetic field components measured by ISEE 2 (the leading satellite). Magnetopause crossings occur in the time intervals denoted by MP1, MP2 and MP3; the magnetopause was defined as the region where B_l is between 90% of its magnetospheric value ($B_{l,\mathrm{msph}} \approx 58$ nT) and 90% of its magnetosheath value ($B_{l,\mathrm{msh}} \approx -45$ nT), that is, it is the layer where the major part of the magnetic field jump takes place. Magnetospheric and magnetosheath intervals are denoted by MSPH and MSH, respectively. (d) Sketch of the motion of the satellites (dot-dashed lines) and the magnetopause (the MP region between the solid lines) whose radial position R measured along the outward normal varies with time. (e–g) Same as Figures 1a–1c. (h) Mean electron density N^- between both spacecraft; a low-pass filter was used to reduce the noise level.

We demarcate the current layer as the region where B_l is between 90% of its magnetospheric value ($B_{l,\mathrm{msph}} \approx 58$ nT) and 90% of its magnetosheath value ($B_{l,\mathrm{msh}} \approx -45$ nT); that is, it is the layer where the major part of the magnetic field jump takes place. The magnetospheric and magnetosheath intervals are denoted by MSPH and MSH, respectively. The three magnetopause crossings are the consequence of the changing position of the magnetopause [e.g., *Holzer et al.*, 1966; *Song et al.*, 1988]. Figure 1d sketches

the motion of the satellites (dot-dashed lines) and the magnetopause (the MP region between the solid lines) whose position R along the N axis varies with time. This sketch obviously reflects the fact that ISEE 2 spends a longer time than ISEE 1 in the MSH region between the MP1 and MP2 crossings, while ISEE 1 spends a longer time than ISEE 2 in the MSPH region between the MP2 and MP3 crossings. It can be seen that the second magnetopause crossing (MP2) is the most rapid one for both satellites. We have assumed that the normal velocity of the magnetopause with respect to both satellites during this event, V_n^{MP2}, is constant. Its value is deduced from the time interval $T_{12} = 11$ s between the reversals of the B_l component (instants when $B_l = 0$) observed successively by ISEE 1 (1448:11) and ISEE 2 (1448:22) and from the component of the separation distance in the normal direction, $D_{12} = 220$ km; we find $V_n^{MP2} = D_{12}/T_{12} = 20$ km/s. From the mean (of the two satellites) duration of the crossing of the MP2 event (≈ 28 s) a magnetopause thickness $D \approx 560$ km is obtained, that is, a value close to the average thickness found near the magnetic equator by *Berchem and Russell* [1982]. With a typical proton Larmor radius in the magnetosheath (ρ^+_{msh}) of 50 km, we conclude that $D \approx 11\rho^+_{msh}$.

Figure 1h displays the integrated electron density N^- between the spacecraft. Local electron density fluctuations are automatically smoothed by measuring the integrated density. The frequencies ranging from $f^* = 1/T_{12}$ (0.09 Hz for the second magnetopause crossing) up to the Nyquist frequency $f_{Nyquist}$ can therefore be ascribed mainly to experimental noise. A low-pass filter with a cutoff frequency $f_{cutoff} = 0.05 f_{Nyquist}$ intermediate between f^* and $f_{Nyquist}$ was used to reduce this noise. The temporal resolution is sufficient to analyze the fine structure of the density profiles across the magnetopause.

Although we have no plasma data other than the electron density, we will approximate the magnetopause at the time of crossing as a tangential discontinuity, since the jump (an increase or a decrease) of the electron density N^-, the change in magnitude and direction of the tangential magnetic field ($\mathbf{B} = \mathbf{B}_t$), and the small normal component of the magnetic field ($\mathbf{B}_n \approx 0$), as seen in Figure 1, are compatible with the Rankine-Hugoniot conditions across a tangential discontinuity [e.g., *Spreiter and Stahara*, 1985]:

$$[N^-] \neq 0, \quad \mathbf{B}_n = 0, \quad [\mathbf{B}_t] \neq 0.$$

3. Fine Structure of the Density Profiles at the Subsolar Magnetopause

The multiple crossing of Figure 1 is studied below in more detail by performing a superposed epoch analysis. Subsequently, the observed electron density overshoot is shown to be consistent with the density profile predicted by a plasma kinetic model. Finally, we discuss the conditions for which theory predicts the presence of such an electron density overshoot.

3.1. Superposed Epoch Analysis

In order to study the variations of the magnetic field and electron number density across the three magnetopause crossings of Figure 1, we perform a superposed epoch analysis of these three crossings as recorded by ISEE 1. Implicit in this analysis is the hypothesis that the magnetopause normal velocity with respect to the satellite is constant during each crossing. This hypothesis can be broken by either strong upstream solar wind pressure variations or fast magnetopause oscillations. As the magnetopause position fluctuates over only a narrow range, the solar wind dynamic pressure variations must have been small. Very fast magnetopause oscillations seem to be absent (see the sketch of the magnetopause motion in Figure 1d). The constant velocity approximation therefore seems reasonable. The superposed epoch analysis appears to be justified, since there is a strong similarity between the individual transitions. We therefore assume that the internal structure of the magnetopause is essentially unaffected by the small solar wind dynamic pressure fluctuations. Figures 2a–2d display respectively the tangential components of the magnetic field B_m and B_l, its magnitude B, and the electron number density N^-, in terms of the x_n coordinate defining the normal distance to the TD plane, oriented outward from the magnetosphere toward the magnetosheath. To translate timescales into spatial scales, we have used our estimate of the thickness (560 km). Because the electron density measured by the wave propagation experiment gives the average value between ISEE 1 and ISEE 2, the temporal scales of the density profile across the three magnetopause crossings illustrated in Figure 1 were first shifted by half the time delay between the instants when $B_l = 0$ as observed successively by the two satellites (this temporal shift is positive for the MP1 and MP3 crossings, and negative for the MP2 crossing). The superposed magnetopause crossings in the left panels of Figure 2 are centered on the dip of the magnetic field magnitude. The MP2 crossing is the key transition from which the timescale has been translated to the spatial scale deduced from the magnetopause thickness estimate. The MP1 and MP3 crossings are superimposed using scaling factors that produce the best superposition of the three crossings. From the superposed epoch analysis it can be seen that the MP events of Figure 1 all are very similar, in particular regarding the height and position of the electron density overshoot. This supports the scenario of the oscillating position of the magnetopause. It does not matter for the present study whether the magnetopause moves collectively, or whether a traveling surface wave leads to a local displacement of the magnetopause only. The spatial scale is expressed in proton Larmor radii in the magnetosheath (ρ^+_{msh}). Since we have no temperature data, ρ^+_{msh} has been computed using a typical value of 300 eV for the proton temperature in the magnetosheath; this value is close to the average temperature of 3.78×10^6 K given by *Phan et al.* [1994] for the protons in the magnetosheath close to a magnetopause with high magnetic shear. With $B_{msh} \approx 50$ nT, one finds $\rho^+_{msh} \approx 50$ km.

Figure 2d shows that the electron density in the MCL is

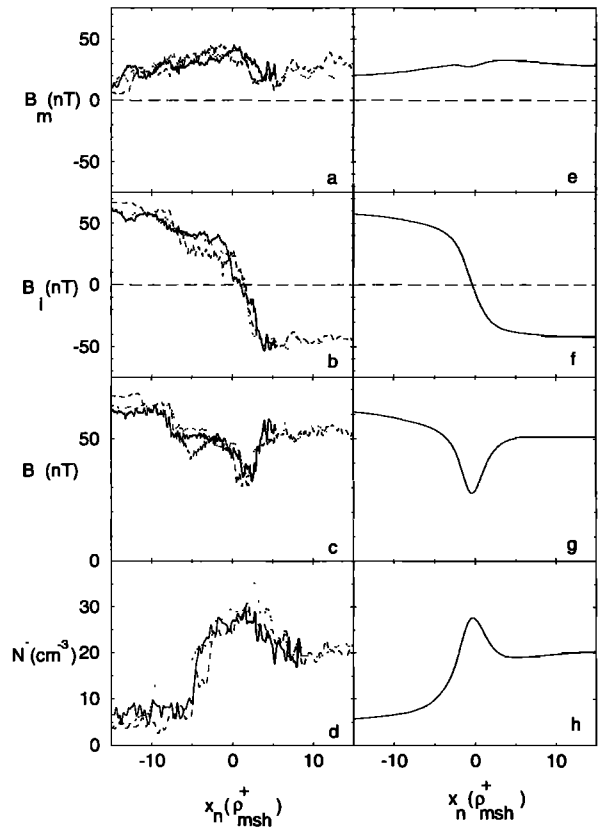

Figure 2. Superposed epoch analysis and theoretical simulation of the ISEE 1 multiple magnetopause crossing observed on August 30, 1981 (day 242). (a–d) Observed tangential magnetic field components B_m and B_l, the magnetic field intensity B, and the average electron density between ISEE 1 and 2, shown in a superposed epoch plot. The basis for the distance scale x_n is an estimate of the magnetopause velocity $V_n^{\mathrm{MP2}} \approx 20$ km/s during the second crossing and a typical magnetosheath ion gyroradius of 50 km. The three crossings have the same overall profile, corroborating the hypothesis of an oscillating magnetopause. (e–h) Results of a simulation by means of a kinetic model. The overall correspondence is good: We find the same magnetic field rotation, the same strength of the depression in the magnetic field inside the transition, and the same magnitude of the electron density overshoot. When comparing Figures 2d and 2h one should bear in mind that Figure 2d represents an averaged electron density between both spacecraft, whose separation distance is about $4\rho^+_{\mathrm{msh}}$; such an averaging leads to a broadening of the observed density peak.

enhanced with respect to the magnetosheath. If N_M^- is the maximum electron density in the MCL, and N_{msh}^- the electron density further in the inner magnetosheath, we obtain a characterizing density factor defined by

$$\delta = (N_M^- - N_{\mathrm{msh}}^-)/N_{\mathrm{msh}}^-.$$

The values of δ corresponding to the three successive crossings of the magnetopause between 1445 and 1452 UT are $\approx$ 0.35, 0.45 and 0.29 while the asymmetry factors are $\kappa_B \approx$ 0.16, 0.16 and 0.22 and the angles of magnetic field rotations are successively 143°, 145° and 146°. Note that it is not easy to define the value of δ precisely; we have used the low-pass filter mentioned earlier to smooth away experimental noise first.

The number of magnetopause crossings for which ISEE 1 and ISEE 2 were sufficiently close to each other and for which the experiment operated in the right mode to yield high-resolution electron density profiles is limited. Table 1 displays the magnetic field parameters (θ,κ_B) and the electron density overshoot δ for five magnetopause crossings with high magnetic shear θ, measured on three ISEE 1-2 orbits. The values of the observed parameters κ_B vary between 0.16 and 0.35. All cases show similar density enhancements with δ between 0.29 and 0.50.

3.2. Theoretical Analysis

The profile of the electron density enhancement in Figure 2d resembles that predicted by the KR model. The KR model, however, describes a simplified kinetic Vlasov equilibrium of tangential discontinuities (TD), where, for example, all electron and proton populations are characterized by a single temperature. We therefore use a more general version of this model [*Roth et al.*, 1996; *De Keyser et al.*, 1996] in order to eliminate some of the simplifications.

Let the coordinates of the satellite in the LMN frame be denoted by x_l, x_m, x_n. In the hypothesis of a locally planar magnetopause, its structure is one-dimensional and can be expressed in terms of the normal coordinate x_n only. The standard procedure for solving the Vlasov equations for charged particles (of mass m and charge Ze) moving in a steady plane TD electromagnetic configuration [e.g., *Longmire*, 1963, chap. 5] consists of first expressing the velocity distribution functions (VDFs) as functions of the constants of motion: the particle's energy H and canonical momenta $\mathbf{p} = (p_l, p_m)$. The next step is to obtain the partial densities and currents as functions of the electrostatic potential ϕ and the vector magnetic potential components a_l and a_m, by integrating the VDFs over velocity space. Finally, Maxwell's equations lead to a set of coupled ordinary differential equations for a_l and a_m, supplemented by the quasi-neutrality condition for ϕ. This set is solved numerically by means of an adaptive step ordinary differential equation integrator.

The model makes a distinction between so-called "outer" and "inner" populations. It considers four pairs of electron and proton populations: the outer and inner magnetospheric populations ($x_n < 0$) and the inner and outer magnetosheath populations ($x_n > 0$).

Table 1. Available High Magnetic Shear Subsolar Tangential Discontinuity Magnetopause Crossings: The Magnetic Field Asymmetry Factor κ_B, the Magnetic Field Rotation Angle θ, and the Electron Density Overshoot δ

Year	Day	Hour, UT	κ_B	θ	δ
1981	242	1446	0.16	143	0.35
1981	242	1448	0.16	145	0.45
1981	242	1450	0.22	146	0.29
1981	245	0105	0.35	157	0.50
1981	278	1308	0.32	162	0.50

The outer (magnetospheric and magnetosheath) populations each have a nonzero density on one side of the transition. The fact that the magnetosheath (magnetospheric) populations penetrate into the magnetosphere (magnetosheath) over only a limited distance implies the presence of a cutoff factor in their VDF: a part of velocity space is inaccessible for particles of magnetosheath (magnetospheric) origin (for a detailed discussion, see *Roth et al.* [1996]). This cutoff factor is parameterized by the transition length $\mathcal{L}$, which gives the typical length scale of variations in the moments of the VDF (density, current, velocity) [*Roth et al.*, 1996; *De Keyser et al.*, 1996, 1997; *De Keyser and Roth*, 1997]; it typically is a few times the gyroradius ρ of a thermal particle in the asymptotic magnetic field ($B_\infty = B_{\mathrm{msph}}$ or B_{msh}, depending on the origin of the population).

An inner population is associated with each outer one. In order to limit the number of parameters, the model requires that an inner population have the same transition length and the same temperature as the corresponding outer population (we will comment on this hypothesis in the discussion). The difference is that an inner population has a nonzero bulk velocity, essentially a drift speed related to the B_l gradient. A consequence of this drift speed is that the inner populations are present only inside the transition, in a layer whose characteristic length scale is $\mathcal{L}_d$; the drift speed of an inner population with temperature T is given by $V_d = 2kT/Ze\mathcal{L}_d B_\infty$ [*Harris*, 1961]. The inner population density at the center of the transition $n_{\mathrm{inner}}(x_n = 0)$ is related to the density of the corresponding outer population at $x_n = 0$ ($n_{\mathrm{outer}}(x_n = 0)$) by a given ratio $\nu = n_{\mathrm{inner}}(x_n = 0)/n_{\mathrm{outer}}(x_n = 0)$ (the "center" of the transition $x_n = 0$ is defined by setting the magnetic potential $a_l(0) = a_m(0) = 0$). Inner ions and electrons have opposite drift speeds, such that there is a net current: the diamagnetic magnetopause current that shields the magnetosphere from the solar wind environment and that causes the rotation of the magnetic field.

Such a Vlasov model has been used to simulate the observed magnetopause crossings. The simulated profiles are displayed in the right panels of Figure 2. The principle is simple: Given the observed boundary conditions on each side of the magnetopause (densities, temperatures, magnetic field) a satisfactory numerical simulation is obtained when suitable parameters for $\mathcal{L}$, $\mathcal{L}_d$ (or equivalently V_d) and ν are found; ν can be found from the pressure balance between the center of the transition and the total pressure outside the magnetopause, and the characteristic lengths should match the length scales of the observed profiles.

Since only the electron number densities and the magnetic field are measured ($N^-_{\mathrm{msph}} = 5\ \mathrm{cm}^{-3}$, $N^-_{\mathrm{msh}} = 21\ \mathrm{cm}^{-3}$, $B_{\mathrm{msph}} = 63$ nT, $B_{\mathrm{msh}} = 51$ nT), assumptions have to be made concerning the plasma temperatures. We choose typical values [*Phan et al.*, 1994]: a magnetosheath proton temperature $T^+_{\mathrm{msh}} = 300$ eV, and temperature ratios $T^+_{\mathrm{msh}}/T^-_{\mathrm{msh}} = 5$ and $T^+_{\mathrm{msph}}/T^-_{\mathrm{msph}} = 10$. The electron temperature in the magnetosheath then is $T^-_{\mathrm{msh}} = 60$ eV. The magnetospheric temperatures then follow from pressure balance: $T^-_{\mathrm{msph}} = 76.7$ eV and $T^+_{\mathrm{msph}} = 767$ eV. The ion gyroradii are $\rho^+_{\mathrm{msph}} = 67.5$ km and $\rho^+_{\mathrm{msh}} = 49.2$ km.

The ion transition lengths used in the simulation are typical (chosen in order to match the observed transition thickness): a few times the ion gyroradius ($\mathcal{L}^+_{\mathrm{msph}} = 4\rho^+_{\mathrm{msph}}$, $\mathcal{L}^+_{\mathrm{msh}} = 4\rho^+_{\mathrm{msh}}$); the electron length is a few times smaller ($\mathcal{L}^+_{\mathrm{msph}}/\mathcal{L}^-_{\mathrm{msph}} = \mathcal{L}^+_{\mathrm{msh}}/\mathcal{L}^-_{\mathrm{msh}} = 4$). The length scales of the inner populations are also of the order of the ion gyroradius ($\mathcal{L}^-_{d,\mathrm{msph}} = \mathcal{L}^+_{d,\mathrm{msph}} = 5.5\rho^+_{\mathrm{msph}}$, $\mathcal{L}^-_{d,\mathrm{msh}} = \mathcal{L}^+_{d,\mathrm{msh}} = 2\rho^+_{\mathrm{msh}}$), corresponding to drift speeds $V^+_d = 65$ km/s, $V^-_d = -6.5$ km/s for the inner magnetospheric particles, and $V^+_d = 120$ km/s, $V^-_d = -24$ km/s for the inner magnetosheath particles. The densities of the four inner populations are fixed by the choice $\nu = 1$, corresponding to the observed magnetic field depression inside the transition.

The right panels of Figure 2 show the result of the simulation to be quite satisfactory, given the simple model, the assumptions that had to be made about the temperatures, and the lack of information about the inner populations. The simulated electron density profile (Figure 2h) agrees well with the observed density overshoot (Figure 2d), except that the latter seems to be wider. This is a consequence of the fact that the densities in Figure 2d are averages over the normal spacecraft separation distance of about 4 ρ^+_{msh}; such averaging necessarily leads to a broadening of the density peak. The simulation is characterized by a magnetic field asymmetry factor $\kappa_B = 0.19$, a magnetic field rotation over $\theta \approx 130°$, and a density overshoot $\delta = 0.33$; all these values are close to the observed ones.

3.3. Discussion

From Figure 2 it can be concluded that the simple kinetic model can explain the overshoot of the density observed near the subsolar magnetopause. To explain this result, we describe some aspects of the theoretical model in more detail.

In the KR model the magnetic field rotation angle θ was shown to be an increasing function of the parameter ν, that is, of the relative number density of the inner populations at $x_n = 0$: A stronger B_l variation implies a larger diamagnetic current, and more inner particles are present. The same is true for the more general model used here. Note that in these models the magnetic field rotation angle θ does not (or not strongly) depend on the drift speed: Larger drift speed corresponds to higher diamagnetic current density, but at the same time the diamagnetic layer is thinner, so that the total current remains the same.

For high magnetic shear there are more inner particles than for low magnetic shear: This explains the overshoot of the number density observed in those cases. In general, an overshoot is expected to be present when the number of inner particles is of the same order as or larger than the number of outer particles.

The exact nature of the density profile depends not only on the number of inner particles but also on the location of the bulk of their distribution inside the transition. This is sketched in Figure 3. In Figure 3a, the layer with inner populations is situated at the center of the transition. Figures 3b

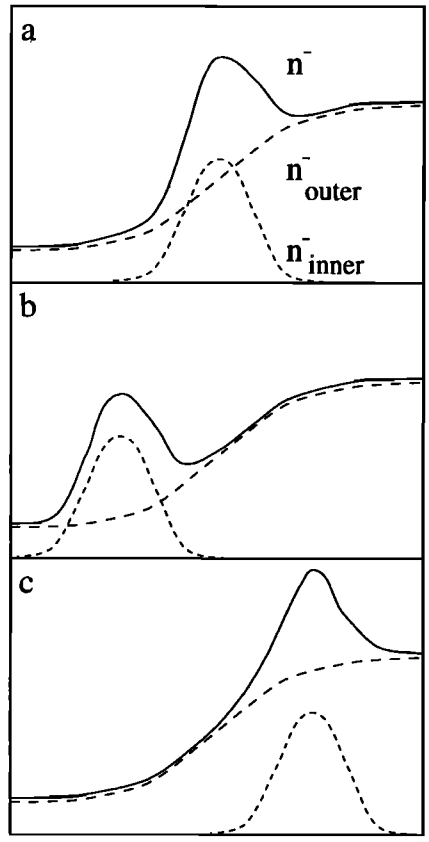

Figure 3. Sketch of the electron density enhancement across the high magnetic shear magnetopause (a) when the drift current layer containing the inner populations is located at the center of the transition, (b) when it is displaced toward the magnetospheric side, and (c) when it is displaced toward the magnetosheath side. The morphology of the total electron density profile is different in each case. The drift current layer displacement should remain small; otherwise, the drift current and the transition between the magnetospheric and magnetosheath plasmas would be unrelated.

and 3c illustrate situations where the layer with inner populations is displaced toward the magnetospheric side and magnetosheath side, respectively. The density profile can have a different morphology, as in Figure 3b which shows a number density depression between the magnetosheath and a plasma bulge located at the magnetospheric side. It is expected, however, that the inner population layer is not displaced too much from the center of the transition. If not, the drift current layer would become completely unrelated to the transition between the magnetospheric and the magnetosheath plasmas. In conclusion, a density overshoot can be expected when the magnetic shear is high.

Figure 4 displays the density enhancement δ versus the magnetic field rotation θ for a fixed value of the magnetic field asymmetry factor $\kappa_B = 0.19$ (the average value for the threefold magnetopause crossing from the superposed epoch analysis). The shaded area in this figure is the locus of magnetopause configurations used in the simulation, allowing for (1) the number density of the inner populations being varied and (2) the position of the diamagnetic layer being possibly shifted away from the center of the transition (such a shift can be obtained by changing the orientation of the drift current in the model). The overall trend is, of course, one of increasing density overshoot with increasing rotation angle. The effect of shifting the diamagnetic layer inside the transition is, however, not unimportant. The circle corresponds to the simulation of Figure 2, the squares with the error bars correspond to the three observed crossings of day 1981/242.

4. Conclusions

For a limited number of cases high time resolution electron density profiles obtained from the ISEE 1-2 propagation density experiment have demonstrated, for the first time, an enhancement of the electron density at the Earth's magnetopause. Because of the limited number of crossings for which high resolution data were available, it was not possible to verify observationally whether such a density enhancement occurs frequently. From the similarity of the in-

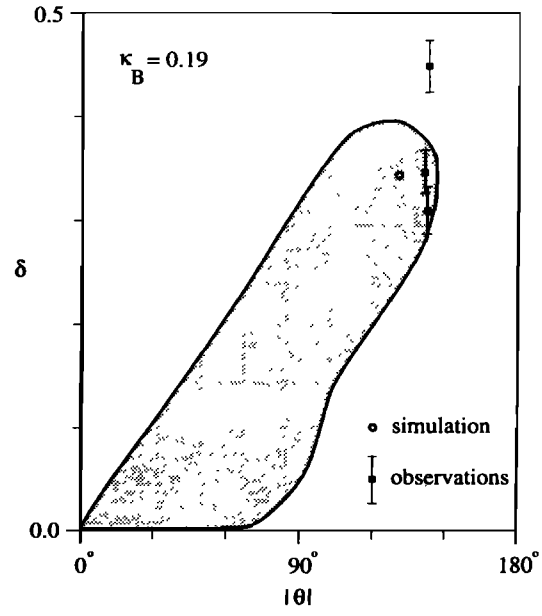

Figure 4. Theoretical variation of δ as a function of the magnetic field rotation angle θ for $\kappa_B = 0.19$, the value used in the simulation of Figure 2. The same plasma temperatures and magnetosheath and magnetospheric temperatures were used as in the simulation; only the number density of the inner populations and the relative position of the inner population layer inside the transition were varied. The shaded band corresponds to the set of possible magnetopause configurations that are obtained in this way. The general trend is that the density overshoot δ increases with the magnetic field rotation angle θ. Deviations from this trend are possible due to the effect of a moderate displacement of the layer containing the inner populations with respect to the center of the transition (see Figure 3). The observed values of δ for the multiple magnetopause crossing of August 30, 1981 (day 242) are indicated by the squares with error bars; the small circle corresponds to the simulation shown in the right panels of Figure 2. There is a good correspondence within the error margins.

dividual transitions in a triple crossing, we infer that the internal structure of the magnetopause does not change dramatically as a consequence of the minor solar wind dynamic pressure fluctuations that are responsible for the small displacements of the magnetopause. The shape of the observed density enhancement is close to that obtained from Vlasov equilibrium models of the tangential discontinuity magnetopause [*Kuznetsova and Roth*, 1995]. We have illustrated this by demonstrating the close correspondence between simulated and observed magnetic field and density profiles.

It should be stressed that very little is actually known about the inner populations. High-resolution plasma observations are of prime importance in resolving the question of the origin and the properties of these inner populations. The one-dimensional TD model used in this study, for instance, does not allow one to trace back the origin of the inner populations [*Whipple et al.*, 1984]. Only models that describe the physical processes responsible for trapping particles inside the current layer can resolve questions related to the temperature of the inner populations, their transition lengths, and the position of the drift current layer inside the transition. In particular, there may be heating at the magnetopause [*Song et al.*, 1993]. The magnetic pressure decrease in the transition in that case may be due to a temperature increase of the inner populations, rather than a density enhancement.

An analysis of the most important parameters in the model shows that an electron density overshoot is expected to be a feature of high magnetic shear configurations: The density peak reflects the presence of a substantial amount of inner particles, which in turn is related to the current responsible for the rotation of the magnetic field. However, such density enhancements do not always occur, and if they do, their magnitude may differ from case to case because of several reasons. As suggested by Figures 3 and 4 the presence of an enhancement depends not only on the magnitude of the magnetic field rotation, but on the position of the drift current layer inside the transition as well. The enhancement will also be smaller or it can even be absent if there is a temperature increase inside the magnetopause. It is therefore not surprising that a density enhancement is not visible in the superposed epoch analysis of *Phan et al.* [1994] (see the high magnetic shear case in their Figure 9) which covers crossings with $|\theta| > 60°$. Also, the low time resolution of the profiles in the superposition may easily obscure details observed within the transition. In the same paper, Phan et al. show examples of crossings with moderate shear with (their Figures 5 and 6, $|\theta| \approx 60°$) and without (their Figure 7, $|\theta| \approx 90°$) a density enhancement. The crossings discussed in the present paper are peculiar because of their very large rotation angle ($|\theta| > 140°$).

The analysis in the present paper ignores the effects of the plasma flow in the magnetosheath. This flow may significantly affect the structure of the transition [*De Keyser and Roth*, 1997]. The analysis therefore is valid only for transitions near the stagnation point.

Acknowledgments. The authors are grateful to C.T. Russell for providing ISEE 1 and 2 magnetic field observations. Part of the work by M.R. was performed during a stay at the Observatoire de Paris-Meudon, France. M.R. thanks the members of the "Département de Recherche Spatiale" for their warm hospitality and stimulating discussions. J.D.K. and M.R. are supported by the ESA (PRODEX) "Ulysses Interdisciplinary Study of Directional Discontinuities", and acknowledge the support of the Belgian Federal Services for Scientific, Technical and Cultural Affairs.

The Editor thanks Christopher T. Russell and another referee for their assistance in evaluating this paper.

References

Berchem, J., and C. T. Russell, The thickness of the magnetopause current layer : ISEE 1 and 2 observations, *J. Geophys. Res., 87*, 2108, 1982.

De Keyser, J., and M. Roth, Equilibrium conditions for the tangential discontinuity magnetopause, *J. Geophys. Res., 102*, 9513, 1997.

De Keyser, J., M. Roth, J. Lemaire, B. T. Tsurutani, C. M. Ho, and C. M. Hammond, Theoretical plasma distributions consistent with Ulysses magnetic field observations in a solar wind tangential discontinuity, *Sol. Phys., 166*, 415, 1996.

De Keyser, J., M. Roth, B. T. Tsurutani, C. M. Ho, and J. L. Phillips, Solar wind velocity jumps across tangential discontinuities: Ulysses observations and kinetic interpretation, *Astron. Astrophys., 321*, 945, 1997.

Harris, E. G., On a plasma sheath separating regions of oppositely directed magnetic fields, *Nuovo Cimento, 23*, 115, 1961.

Harvey, C. C., J. Etcheto, Y. de Javel, R. Manning, and M. Petit, The ISEE electron density experiments, *IEEE Trans. Geosci. Electron., GE-16*, 231, 1978.

Holzer, R. E., M. G. McLeod, and E. J. Smith, Preliminary results from the OGO 1 search coil magnetometer: Boundary positions and magnetic noise spectra, *J. Geophys. Res., 71*, 1481, 1966.

Kuznetsova, M. M., and M. Roth, Thresholds for magnetic percolations through the magnetopause current layer in asymmetrical magnetic fields, *J. Geophys. Res., 100*, 155, 1995.

Lee, L. C., and J. R. Kan, A unified kinetic model of the tangential magnetopause structure, *J. Geophys. Res., 84*, 6417, 1979.

Longmire, C. L., *Elementary Plasma Physics*, Wiley-Interscience, New York, 1963.

Phan, T.-D., G. Paschmann, W. Baumjohann, N. Sckopke, and H. Lühr, The magnetosheath region adjacent to the dayside magnetopause: AMPTE/IRM observations, *J. Geophys. Res., 99*, 121, 1994.

Roth, M., Structure of tangential discontinuities at the magnetopause: The nose of the magnetopause, *J. Atmos. Terr. Phys., 40*, 323, 1978.

Roth, M., A microscopic description of interpenetrated plasma regions, in *Magnetospheric Boundary Layers*, edited by B. Battrick and J. Mort, *Eur. Space Agency Spec. Publ., ESA-SP 148*, 295–309, 1979.

Roth, M., J. De Keyser, and M. M. Kuznetsova, Vlasov theory of the equilibrium structure of tangential discontinuities in space plasmas, *Space Sci. Rev., 76*, 251, 1996.

Russell, C. T., The ISEE 1 and 2 fluxgate magnetometers, *IEEE Trans. Geosci. Electron., GE-16*, 239, 1978.

Russell, C. T., and R. C. Elphic, ISEE observations of flux-transfer events at the dayside magnetopause, *Geophys. Res. Lett., 6*, 33, 1979.

Song P., R. C. Elphic, and C. T. Russell, ISEE 1 and 2 observation of the oscillating magnetopause, *Geophys. Res. Lett., 15*, 744, 1988.

Song, P., C. T. Russell, J. T. Gosling, M. F. Thomsen, and R. C. Elphic, Observation of the density profile in the magnetosheath near the stagnation streamline, *Geophys. Res. Lett., 17*, 2035, 1990.

Song P., C. T. Russell, and M. F. Thomsen, Slow mode transition in the front side magnetosheath, *J. Geophys. Res., 97*, 8295, 1992.

Song P., C. T. Russell, and C. Y. Huang, Wave properties near the subsolar magnetopause: Pc 1 waves in the sheath transition layer, *J. Geophys. Res., 98*, 5908, 1993.

Spreiter, J. R., and S. S. Stahara, Magnetohydrodynamic and gasdynamic theories for planetary bow waves, in *Collisionless Shocks in the Heliosphere: Reviews of Current Research*, edited by B. T. Tsurutani and R. G. Stone, *Geophys. Monogr. Ser. vol. 35*, pp. 85–107, AGU, Washington, D.C., 1985.

Whipple, E. C, J. R. Hill, and J. D. Nichols, Magnetopause structure and the question of accessibility, *J. Geophys. Res., 89*, 1508, 1984.

Zhang, X. X., P. Song, S. S. Stahara, J. R. Spreiter, C. T. Russell, and G. Le, Large scale structure in the magnetosheath: Exogenous or endogenous in origin?, *Geophys. Res. Lett., 23*, 105, 1996.

J. De Keyser and M. Roth, Belgian Institute for Space Aeronomy, Ringlaan 3, B-1180 Brussels, Belgium. (e-mail: Johan.DeKeyser@oma.be, Michel.Roth@oma.be)

C.C. Harvey and D. Hubert, Département de Recherche Spatiale, Observatoire de Paris–Meudon, 5 place Jules Janssen, F-92195 Meudon Cedex, France. (e-mail: chris.harvey@obspm.fr, daniel.hubert@obspm.fr)

(Received April 17, 1997; revised October 31, 1997; accepted November 3, 1997.)